Causal-based Optimization of Micro-Perforated Partitions

Cédric Maury, Teresa Bravo

16ème Congrès Français d'Acoustique
11-15 Avril 2022, Marseille

Causal-based Optimization of Micro-Perforated Partitions

C. Maury [a] et T. Bravo [b]

[a] Aix-Marseille Univ., CNRS, Centrale Marseille,
Laboratoire de Mécanique et d'Acoustique (LMA), Marseille, France
[b] Consejo Superior de Investigaciones Cientificas (CSIC), Instituto de la Tecnologias Fisicas y de la Informacion (ITEFI), Serrano 144, 28006 Madrid, Spain

Acoustic optimization of micro-perforated absorbers is generally achieved by maximizing the total energy dissipated over a frequency band. However, there is a low frequency limit, determined by the principle of causality, below which a broadband absorber will dissipate little energy. In this study, an integral causal relationship is derived in the case of a single-layer micro-perforated resonator (MPR) under normal incidence. It shows that the ultimate broadband performance of the absorber is quantified by the reflected intensity in logarithmic scale integrated over all the positive wavelengths and is upper bounded by the cavity depth. A sensitivity study led to the proposal of a causal optimization criterion in order to obtain the MPR constitutive parameters which provide the broadest possible performance while ensuring total absorption at the MPR Helmholtz resonance. This criterion maximizes the directional gradient of the total intensity with respect to the MPR parameters and is readily implemented using a quadrature method and a global optimization solver. It is an alternative to maximizing the total absorption with the advantage of ensuring a critical coupling condition at resonance. This criterion has been extended to the case of general incidence and to a serial arrangement of MPRs. Impedance tube measurements validated the approach, but also showed its limitations for thin elastic structures.

1 Introduction

Environmental noise constitutes a major concern affecting people health and quality of life [1]. In particular, improvement of acoustic absorption and sound insulation at low frequencies using structures with limited size or weight presents a long-standing engineering challenge in the field of noise control. Porous and fibrous absorbers show good broadband performance in the high frequency range, but optimal solutions for low frequency problems are too thick and not suitable to large-scale applications [2, 3]. Micro-Perforated Panels (MPPs) are alternative solutions [4, 5] for situations when porous components are excluded due, for instance, to the presence of a mean flow. However, as they are Helmholtz-type resonators, they provide important absorption properties but confined in a narrow frequency band.

To overcome this difficulty, several solutions have been proposed to enhance the control frequency domain, such as the use of multi-layer configurations deeply studied in the literature [6]. The optimal layout sequences are found by computing the resonance frequencies of the resulting acoustic system, improving the sound absorption bandwidth but at the expense of the increase of the total thickness of the sound absorber. Another similar approach is to use arrangements of multiple MPPs with a multidepth cavity with partitioned sections [7]. Although MPPs can be designed according to specific absorption characteristics by the proper selection of the physical constitutive parameters, the combinatorial optimization problem is not straightforward to solve by conventional techniques and requires the use of random optimization methods [8].

Optimization of one-port acoustical absorbers such as micro-perforated wall-mounted treatments in room acoustics usually has been posed as the maximization of the total absorption averaged over a given frequency band. However, the optimized resonance absorbers achieve a compromise between the peak absorption value, the half-bandwidth frequency range and their overall thickness. An alternative cost function is assessed in this study based on the causality principle in order to maximize over a broad bandwidth the sound power dissipated by a single-layer micro-perforated resonator (MPR) while reaching unit absorption at the Helmholtz resonance.

This problem has already been studied in the field of electromagnetism for the maximization of the bandwidth that can be obtained by radar slab absorbers with a limited thickness. Considering the Bode-Fano result [9, 10] providing the optimal bandwidth achieved by an electronic matching network to transfer power, Rozanov [11] formulated an integral relation between the logarithm of the reflectance magnitude to the thickness of the slab. These results have been extrapolated to the field of acoustics for the design of wideband ultrasonic matching structures made up of two-port multi-layered materials [12]. The integral relations related the reflection transmission coefficients of the matching structure as a function of its effective mass, bulk modulus and of the surrounding media impedances. Other works have investigated the lower bound on the thickness of a rigidly-backed acoustic absorber associated to its effective absorption bandwidth [13]. In this paper we will present a causal-based integral relation to maximize the absorption bandwidth of the sound power dissipated by a single-layer MPR. The paper is organized as follows: the causal-based integral inequality is formulated in Section 2. Section 3 derives the causal optimization criterion of a MPR under normal and general incidence. Section 4 validates these results and provide their extension to double-layer MPRs. Last section summarizes the main conclusions.

2 The causality constraint of a MPR

One considers a rigidly-backed MPR under normal incidence, as shown in Fig. 1, made up of a micro-perforated panel (MPP) backed by a cavity of depth D .

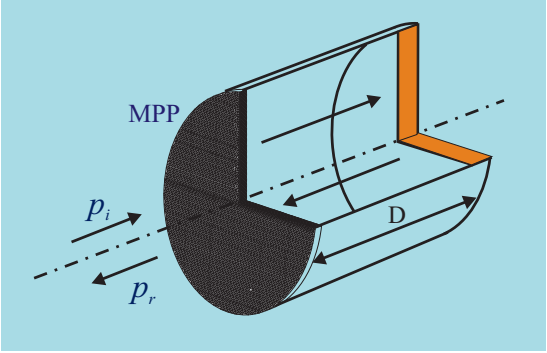

Figure 1 – Schema of single-layer rigidly-backed MPR under normal incidence.

The MPP is characterized by d, the holes diameter, $\sigma = \pi d^2/(4\Lambda^2)$ the perforation ratio, Λ the holes pitch and t the panel thickness.

Causality implies that the back-scattered pressure $p_r(t)$ depends on the incident pressure $p_i(t')$ at earlier times $t' < t$ through the system backscattering response $r(\tau)$, such that $r(\tau) = 0$ for $\tau = t - t' < 0$, as follows

$$p_r(t) = \int_0^\infty r(\tau) p_i(t-\tau)\,\mathrm{d}\tau . \tag{1}$$

Denoting $X(\lambda) = \int_{-\infty}^{\infty} x(\tau)\mathrm{e}^{-2\mathrm{i}\pi c_0 \tau/\lambda}\,\mathrm{d}\tau$ the Fourier wavelength transform of $x(\tau)$, one gets from Eq. (1) the input-output relationship $P_r(\lambda) = R(\lambda)\,P_i(\lambda)$. From the causality principle, $R(\lambda)$ is analytic in the upper-half of the complex wavelength plane and may have a numerable set of zeros in the upper half-plane of complex λ, denoted λ_n, as indicated in Fig. 2.

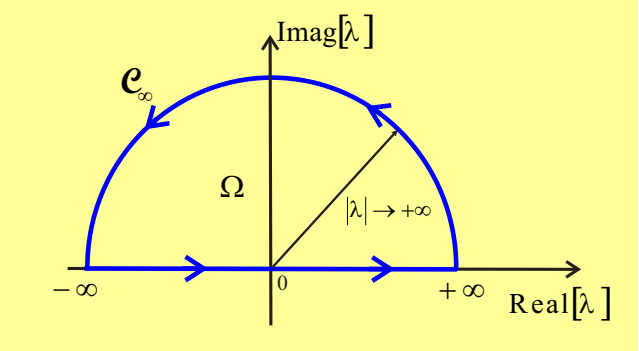

Figure 2 – Representation of the closed contour in the complex wavelength plane.

Following Rozanov's derivation [11], an ancillary function $R'(\lambda)$ is built as follows,

$$R'(\lambda) = R(\lambda)\prod_{n=1}^{\infty}\frac{\lambda-\overline{\lambda}_n}{\lambda-\lambda_n}. \tag{2}$$

$R'(\lambda)$ is analytic and has no poles nor zeros in the upper half-plane of complex λ, as well as $\log(R'(\lambda))$. Cauchy's theorem thus ensures that the integral of $\log(R')$ over any closed contour C within the upper half-plane is zero, e.g. $\oint_C \log(R')\,\mathrm{d}\lambda = 0$, where C can be chosen as an interval over the real wavelengths axis, plus a closing semi-circle of radius $|\lambda|$ in the upper half-plane, as sketched in Fig. 2. Letting $|\lambda| \to \infty$ and taking the real part of the closed-contour integral, one gets

$$2\int_0^\infty \log(|R|)\,\mathrm{d}\lambda = -\mathrm{Real}\left[\int_{C_\infty}\log(R)\,\mathrm{d}\lambda\right] + 2\pi\sum_{n=1}^{\infty}\mathrm{Imag}(\lambda_n) \tag{3}$$

with $\mathrm{Imag}(\lambda_n) > 0$, so that the second term in the right-hand side of Eq. (3) is always positive.

At low frequencies, the input impedance of a MPR can be written as

$$Z(\omega) = \frac{\mathrm{i}m}{\omega}\left[\omega^2 - \omega_H^2 - \mathrm{i}\omega\frac{\xi t}{m}\right], \tag{4}$$

where $m = \rho_0 t k_m/\sigma$ is the effective mass of the MPP with $k_m \approx 1 + (8/3\pi)d/t$ a reactive end-correction factor. $\omega_H^2 = \rho_0 c_0^2/(m d_g)$ is the MPR Helmholtz resonance frequency and $\xi = 32\eta k_r/(\sigma d^2)$ is the MPR resistive term dependent on k_r, a resistive end-correction factor [4]. ρ_0 is the air density and c_0 is the sound speed in air. At low-frequencies, one gets the approximation $\log(R) \approx -4\mathrm{i}\pi c_0 Z_0/(\lambda m \omega_H^2)$ of the plane wave reflection coefficient $R = (Z - Z_0)/(Z + Z_0)$ with $Z_0 = \rho_0 c_0$. The first term in the right-hand side of Eq. (3) then reads $4\pi^2 D$. Eq. (3) then reduces to the following causality constraint

$$\frac{1}{2\pi^2}\left|\int_0^\infty \log(|R|)\,\mathrm{d}\lambda\right| \le D . \tag{5}$$

Assuming $\lambda_{\min} = 0$, Eq. (5) implies that a 90% absorption coefficient requires a MPR whose thickness is greater than $c_0/(17 f_{\min})$. So, $f_{c,\min} = c_0/(17D)$ is a cut-off frequency below which a wideband MPR will exhibit poor absorption performance.

3 The causal optimization criterion

3.1 The causal identity

Setting $Z(\lambda) = Z_0$ and $k_r = 1$, one gets the following exact expression for the zeros of the MPR reflection coefficient:

$$\lambda_0^{\pm} = \pm\frac{2\pi}{k_H^2}\sqrt{k_H^2 - b^2} + \frac{2\mathrm{i}\pi b}{k_H^2}, \tag{6}$$

with $b=0.5(\rho_0/m)(1-\xi t/Z_0)$ and $k_H=\omega_H/c_0$ or equivalently, $2\pi/\lambda_H$. Inserting Eqs. (6) into Eq. (3) yields to the following causal relation for a MPR under normal incidence

$$T(d,\Lambda,t)=\begin{cases} D\dfrac{\xi t}{Z_0} & \text{if} \quad \xi t<Z_0 \\ D & \text{otherwise} \end{cases}, \qquad (7)$$

where $T(d,\Lambda,t)=-(2\pi^2)^{-1}\int_0^\infty \log(|R|)\mathrm{d}\lambda$ is the total intensity reflection coefficient (in logarithmic scale) integrated over all the positive wavelengths. Figure 3 provides a figure of merit for the minimum cavity depth required to build the necessary absorption properties of the MPR over all the positive wavelengths.

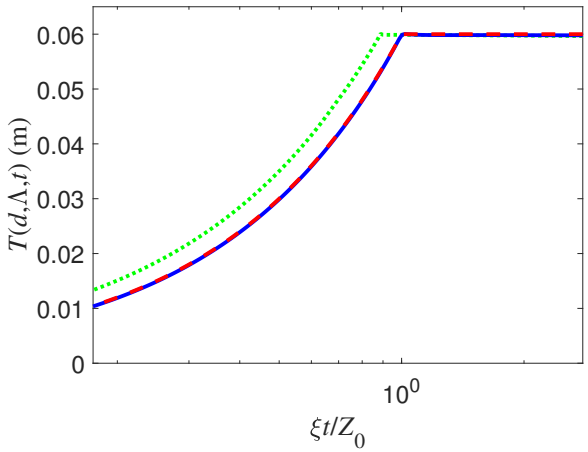

Figure 3 – Variations of $T(d,\Lambda,t)$ as a function of $\xi t/Z_0$: assuming $k_r=1$ (exact expression, blue; numerical quadrature, red) and when accounting for the Rayleigh-type outer resistive end-correction [4], (green).

It can be seen that T equates D when $\xi t>Z_0$ and decays as $\xi t/Z_0$ when $\xi t<Z_0$. If $\xi t=Z_0$, impedance matching occurs and the total amount of energy entering the MPR apertures is fully dissipated by the viscous losses within the holes and at their inlet/outlet. The same trend is observed if one accounts for the outer resistive end-corrections, although downshifted due to the added damping.

3.2 The optimization criterion

When the specific resistance $r=\xi t/Z_0$ decreases towards unity, e.g. when $|R(\lambda)|$ tends to be zero-valued while approaching λ_H from the lower non-causal half-plane, $\partial T/\partial d$ is zero-valued if $r>1$. In this regime, the MPR reaches its ultimate wideband performance, $T=D$, and is insensitive to variations of the MPP parameters [Fig. 4(a)]]. In the other regime, when r increases towards unity, the sensitivity function, $\partial T/\partial d=-4rD/d$, reaches a maximum value at $r=1$, e.g. when $|R(\lambda)|$ tends to be zero-valued while approaching $\lambda=\lambda_H$ from the upper-causal half-plane. The maximum sensitivity of T is thus reached [Fig. 4(b)] for an optimal value of the MPP holes diameter, $d=d_{\text{opt}}$, at which the MPR achieves perfect absorption at its resonance [Fig. 4(c)], thus leading to the following causal-based criterion,

$$d_{\text{opt}}=\arg\max_d\left|\frac{\partial T}{\partial d}\right|. \qquad (8)$$

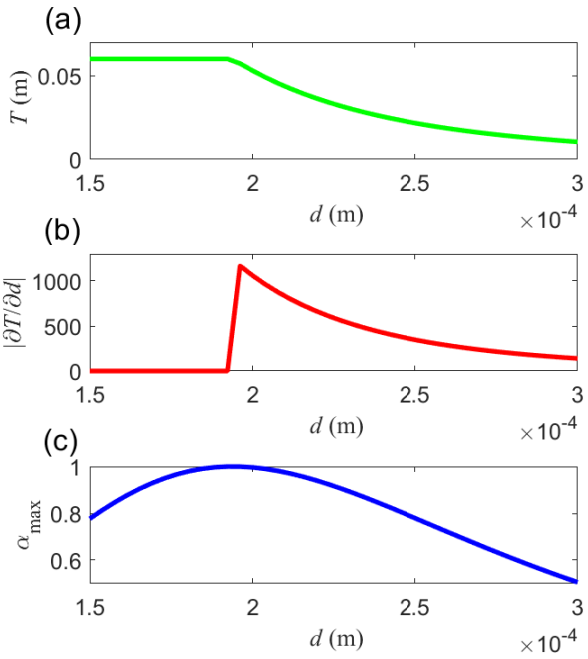

Figure 4 – Variations of $T(d,\Lambda,t)$ (a), $|\partial T/\partial d|$ (b) and the absorption peak value $\alpha_{\max}$ as a function of d.

3.3 Extension to a general incidence

The criterion given by Eq. (8) can be generalized to the case of an oblique incident plane wave impinging onto a MPR with an angle θ_0 with respect to the normal to the MPP surface. The MPR Helmholtz resonance frequency then scales on $1/\cos(\theta_0)$ due to increased apparent stiffness of the air cavity. The MPP surface impedance has to match $Z_0/\cos(\theta_0)$, for the reflexion coefficient R_{θ_0} to be zero-valued. Following the same rationale than in Sec. 3.1 and Sec. 3.2, the following causal relation is obtained for a MPR under general incidence,

$$T_{\theta_0}=\begin{cases} Dr\cos^2(\theta_0) & \text{if} \quad r\cos(\theta_0)<1 \\ D\cos(\theta_0) & \text{otherwise} \end{cases}, \qquad (9)$$

with $T_{\theta_0}(d,\Lambda,t) = -(2\pi^2)^{-1}\int_0^\infty \log\left(\left|R_{\theta_0}\right|\right)\mathrm{d}\lambda$. Figure 5 shows that, when θ_0 increases towards grazing incidence, one observes an increase of the optimal MPP flow resistance, $r = 1/\cos(\theta_0)$, at which the MPR achieves perfect absorption.

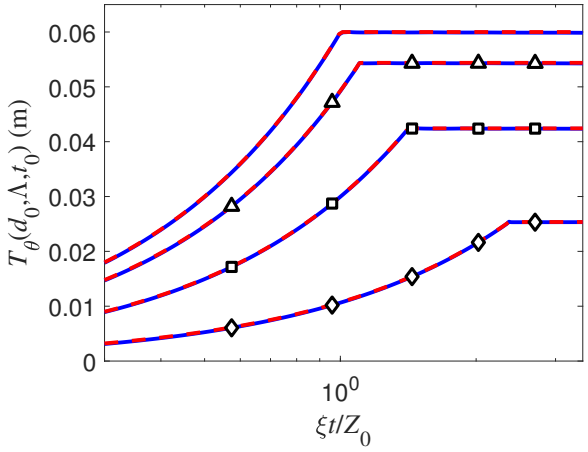

Figure 5. Influence of the incidence angle θ_0 ($\theta_0 = 0°$, black solid; $\theta_0 = 25°$, triangle; $\theta_0 = 45°$, square; $\theta_0 = 65°$, diamonds) on the causality integral T_{θ_0} with respect to the MPP specific flow resistance $\xi t/Z_0$ (exact, red dashed; numerical quadrature, blue solid).

4 Applications

4.1 Experimental validation of the causal-based design of a single-layer MPR

Figure 6(a) shows the effect of the MPP holes diameter on $T(d,\Lambda,t)$ when considering a MPR with cavity depth $D = 60\,\mathrm{mm}$. The fixed MPP parameters are indexed by 0, e.g. the holes pitch, $\Lambda_0 = 5\,\mathrm{mm}$, and the MPP thickness, $t_0 = 0.5\,\mathrm{mm}$. An optimal value, $d_{\mathrm{opt}} = 0.42\,\mathrm{mm}$, has been found from maximizing the sensitivity of the total reflected intensity T with respect to d, e.g. from $d_{\mathrm{opt}} = \arg\max_d \left|\partial T/\partial d\right|$, [see Eq. (8)]. In relation to Eq. (7), when d increases up to d_{opt} ($r > 1$), the absorption half-bandwidth decreases, but the absorption peak value increases by an amount such that $T(d,\Lambda_0,t_0)$, the total intensity reflection integrated over all wavelengths, stays constant equal to D. When d increases above d_{opt} ($r < 1$), both the absorption half-bandwidth and peak value decrease. When $d = d_{\mathrm{opt}}$ ($r = 1$), perfect absorption, also termed critical coupling, occurs at the MPR Helmholtz resonance, e.g. the total amount of energy entering the MPR through the MPP perforations is fully dissipated by the viscous losses within the holes and at their inlet/outlet.

Figure 6(b) compares the absorption spectra of two MPRs that only differ by their holes diameter values, reduced from $d = 0.5\,\mathrm{mm}$ in the nominal configuration (blue, $r < 1$) down to $d_{\mathrm{opt}} = 0.42\,\mathrm{mm}$ in the optimal configuration (red, $r = 1$). The nominal and optimal MPPs have been manufactured by mechanical drilling an aluminium disk of overall diameter 0.1 m. Their absorption properties were measured in a standing wave tube in plane wave regime using the two-microphone method up to the duct cut-on frequency of 2.1 kHz. The simulations and the measurements shown in Fig. 6(b) are in good agreement in both the nominal and optimal configurations. They confirm a broadband spectrum of the optimal MPR with near unit absorption peak value at its Helmholtz resonance frequency at 606 Hz. Extra absorption peaks however appear due to the effect of the panel volumetric resonances, not accounted for in the model that assumes a rigid MPP.

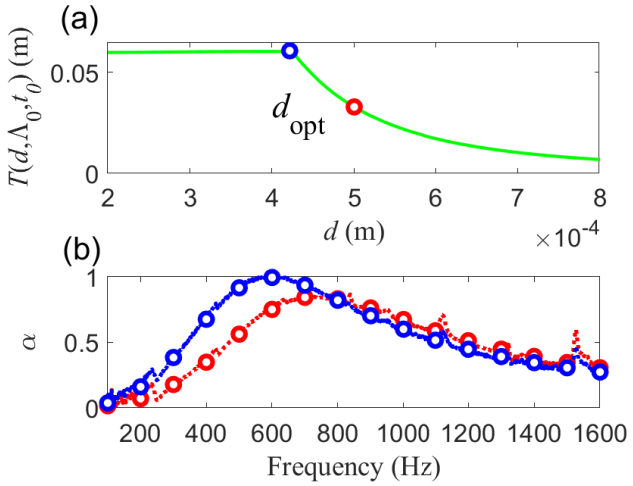

Figure 6. (a) Influence of the MPP holes diameter on the causality integral of a single layer MPR; (b) the corresponding absorption coefficient spectra assuming a MPR with optimized holes diameter so that $r = 1$ (blue) and a nominal MPR with $r < 1$ (red): Kundt tube absorption measurements (dots) and simulations (circles).

4.2 Extension to a double-layer MPR

Following the same rationale than in Sec. 2, the following causal relation can be established for a double-layer MPR made up of MPP1 with holes diameter d_1, holes pitch Λ_1 and thickness t_1 separated by a cavity of depth D_1 from MPP2 with parameters d_2, Λ_2 and t_2, itself separated from a rigid backing wall by a cavity of depth D_2. It reads

$$\left|T_2\right| \le D_1 + D_2\,, \tag{10}$$

with $T_2(d_i,\Lambda_i,t_i) = -(2\pi^2)^{-1}\int_0^\infty \log(|R|)\mathrm{d}\lambda$, $i=1,2$.

Assuming a double-layer MPR, causal-based search for the optimal values of MPP holes diameters that achieve resonant states with unit absorption is carried out using the following criterion

$$(d_1,d_2) = \arg\max_{(d_1,d_2)} \left\| \mathbf{grad}_{(d_1,d_2)}(T) \right\|_2, \qquad (11)$$

using constrained particle swarm optimization solver. The MPR fixed parameters are the holes pitch, $\Lambda_1 = 2.3\,\mathrm{mm}$ for MPP1, $\Lambda_2 = 6.8\,\mathrm{mm}$ for MPP2, the panel thicknesses $t_1 = t_2 = 0.2\,\mathrm{mm}$ and the cavity depths $D = 60\,\mathrm{mm}$ and $D = 30\,\mathrm{mm}$. After maximizing criterion (11), a global optimum $(d_{1,\mathrm{opt}}, d_{2,\mathrm{opt}}) = (0.24\,\mathrm{mm}, 0.39\,\mathrm{mm})$ is obtained. For these parameters, the MPR has two resonant states with unit absorption associated to maximum air particle velocity on the front MPP1: one at $f_1 = 500\mathrm{Hz}$, the Helmholtz frequency of MPP1 rigidly backed by the overall cavity of depth $D_1 + D_2$, and another one at $f_2 = 970\mathrm{Hz}$, the Helmholtz frequency of MPP1 backed by MPP2, as seen in Figure 7. Figure 7 shows that this solution is very close to that obtained after maximizing the total absorption $\overline{\alpha}_0$ over the full range of parameters (d_1,d_2), but the latter strategy does not necessarily provide solutions with unit absorption.

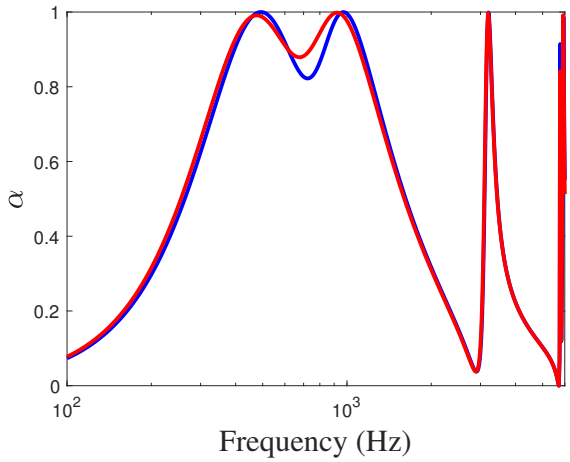

Figure 7. Variations in the (d_1,d_2) plane of the MPR absorption spectra when maximizing the causal criterion (blue) and $\overline{\alpha}_0$ (red) over the full range of (d_1,d_2) parameters.

5 Conclusions

A causal-based integral relationship has been derived for a single-layer rigidly-backed MPR under normal incidence. It shows that the ultimate wideband performance of the MPR, that integrates contributions of the intensity reflection coefficient over all the positive wavelengths, is upper bounded by the absorber cavity depth. It has been extended to general incidence and double-layer MPRs.

A causal-based optimization criterion has been obtained that maximizes the sensitivity of the total reflected intensity with respect to the MPP constitutive parameters. It provides optimal MPRs with maximum wideband performance, able to achieve perfect absorption at their Helmholtz resonance frequency. It has been used to guide the experimental design of single-layer MPRs to ensure they achieve unit absorption at their Helmholtz frequency.

Acknowledgments

This work has been funded by The Ministerio de Economía y Competitividad in Spain, project TRA2017-87978-R, AEI/FEDER, UE, and the mobility program ILINK+2018. It was supported in France by the ANR VIRTECH (ANR-17-CE10-0012-01).

References

[1] U. Ingard. Noise Reduction Analysis. Jones and Bartlett Publishers, Sudbury, Massachusetts (2010).

[2] C. Zwikker and C. W. Kosten, Sound Absorbing Materials, Amsterdam, Elsevier Press (1949).

[3] T.J. Cox and P. D'Antonio, Acoustic absorbers and diffusers – Theory, Design and Application, Spon Press (2004).

[4] D. Y. Maa, Potential of microperforated panel absorbers, Journal of the Acoustical Society of America 104, 2861–2866 (1998).

[5] D. Y. Maa, Microperforated-panel wideband absorbers, Noise Control Engineering Journal 29, 77–84 (1987).

[6] C. Wang and L.H. Huang. On the acoustic properties of parallel arrangement of multiple micro-perforated panel absorbers with different cavity depths, Journal of the Acoustical Society of America 130(1), 208-218 (2011).

[7] N. N. Kim and J. S. Bolton, Optimization of multi-layer microperforated systems for absorption and transmission loss, NoiseCon'14, Advancing the Technology and Practice of Noise Control Engineering, Florida, United States, 8-10 September (2014).

[8] T. Bravo, C. Maury and C. Pinhède, Enhancing sound absorption and transmission through flexible multi-layer micro-perforated structures, Journal of the Acoustical Society of America 134(5), 3663–3673 (2013).

[9] R. M. Fano, Theoretical limitations on the broadband matching of arbitrary impedances, J. Franklin Inst. 249, 57–83 (1950).

[10] H. W. Bode, Network Analysis and Feedback Amplifier Design, Princeton, Van Nostrand, New-Jersey, (1945).

[11] K. N. Rozanov, Ultimate Thickness to Bandwidth Ratio of Radar Absorbers, IEEE Trans. Ant. Propag. 48, 1230–1234 (2000).

[12] O. Acher, J. M. L. Bernard, P. Maréchal, A. Bardaine, F. Levassort, Fundamental constraints on the performance of broadband ultrasonic matching structures and absorbers, J. Acoust. Soc. Am. 125,1995-2005 (2009).

[13] M. Yang, S. Chen, C. Fu, P. Sheng, Optimal sound-absorbing structures, Mater. Horiz. 4, 673–680 (2017).